Journal of Alloys and Compounds 505 (2010) 523–526

Contents lists available at ScienceDirect

Journal of Alloys and Compounds

journal homepage: www.elsevier.com/locate/jallcom

Review

Study of Cu, Co, Mn and La doped NiZn ferrite nanorods synthesized by the coprecipitation method

Qiaoling Li[a,*], Yongfei Wang[b], Chuanbo Chang[a]

[a] Department of Chemistry, School of Science, North University of China, Taiyuan 030051, China
[b] The Thirty-third Research Institute, China Electronics Technology Group Corporation, Taiyuan 030006, China

ARTICLE INFO

Article history:
Received 27 January 2010
Received in revised form 16 June 2010
Accepted 22 June 2010
Available online 1 July 2010

Keywords:
Inorganic compounds
Electron microscopy
Magnetic properties
X-ray diffraction

ABSTRACT

The Zn- and Ni-doped spicular α-FeOOH precursor sample was obtained by coprecipitation-air oxidation method. The $Ni_{0.5}Zn_{0.5}Fe_2O_4$ nanorods with an average diameter of 40 nm and an aspect ratio of 20 were prepared after the calcination process for maintaining the morphology of α-FeOOH precursor. Cu, Co, Mn and La were doped into $Ni_{0.5}Zn_{0.5}Fe_2O_4$ to prepare $Ni_{0.4}M_{0.1}Zn_{0.5}Fe_2O_4$ (M represents Cu, Co, Mn, La) nanorods. The phase, morphology and particle diameter of the samples were studied by X-ray diffraction (XRD) and transmission electron microscopy (TEM). The results showed that the aspect ratio of the $Ni_{0.4}M_{0.1}Zn_{0.5}Fe_2O_4$ decreased with an increase in the absolute difference of the radius of the dopant ion and Fe^{2+}. Therefore, the aspect ratio of the $Ni_{0.4}Cu_{0.1}Zn_{0.5}Fe_2O_4$ nanorods obtained by doping Cu was maximal and the value was higher than 25. The magnetic properties were measured using a vibrating sample magnetometer (VSM), which indicated that the coercivity of the $Ni_{0.4}M_{0.1}Zn_{0.5}Fe_2O_4$ sample decreased and the magnetization increased with an increase in the calcination temperature. The higher anisotropy due to the rod-like structure of the ferrites is responsible for the superior magnetic properties obtained in the present work compared to those reported for ferrites with irregular grain shapes.

Contents

1. Introduction

Spinel ferrites, MFe_2O_4 (M = Mg, Mn, Fe, Co, Ni, Zn, Cu, Cd, etc.) are a technologically important group of materials owing to their diverse applications in high-density magnetic recording, ferrofluids technology, biomedical drug delivery and magnetic resonance imaging (MRI) [1–4]. In recent years, considerable attention has been focused on the one-dimensional nano-sized particles of different ferrites because they could provide versatile building blocks for fabricating functional nanoscale electronic, optoelectronic, photonic, chemical and biomedical devices based on the bottom-up paradigm [5,6]. As a result, the synthesis of one-dimensional nanostructured spinel magnetic materials has become particularly important in the research of the magnetic materials.

In addition, it is very important to control the electrical resistivity and the magnetic properties of the ferrite in many applications. For this purpose, two major possibilities are available: controlling the sintering temperature and atmosphere or adding some additives or substituents. Farea [7], Ashiq [8] and Shobanaa [9] studied the substitution of dopant cations into the spinel structure. Their investigation showed a modification and improvement of the basic electrical and magnetic properties due to the substitution of iron with dopant cations.

Various techniques such as sol–gel [10], coprecipitation [11], hydrothermal [12], combustion reaction [13], mechano-chemical [14], precursor [15] and micro-emulsion [16] methods have been

* Corresponding author. Tel.: +86 351 3923197; fax: +86 351 3922152.
E-mail address: qiaolingl@163.com (Q. Li).

0925-8388/$ – see front matter © 2010 Elsevier B.V. All rights reserved.
doi:10.1016/j.jallcom.2010.06.132

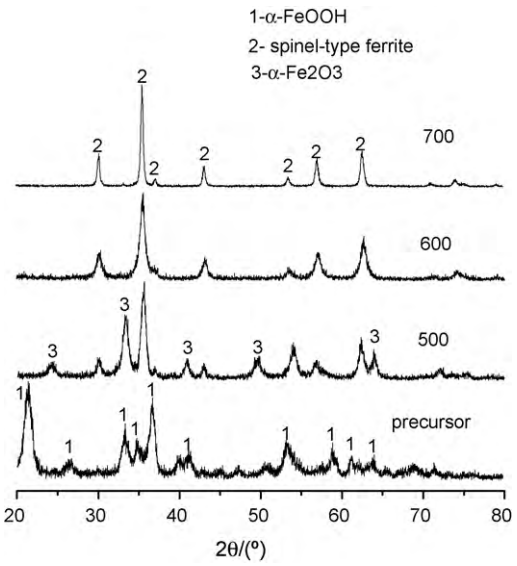

Fig. 1. The XRD pattern of Cu-doped precursor and $Ni_{0.4}Cu_{0.1}Zn_{0.5}Fe_2O_4$ samples obtained at different calcinations temperatures.

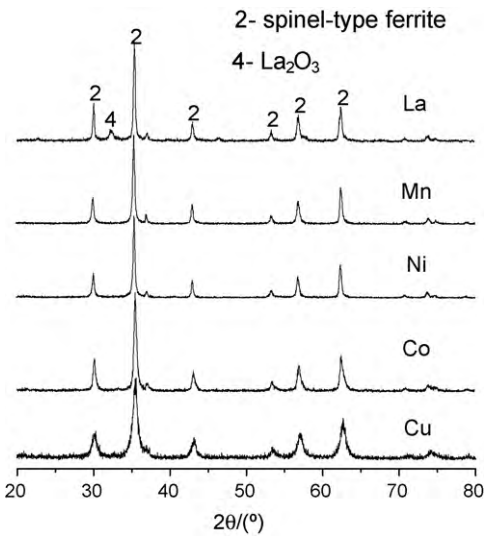

Fig. 2. The XRD spectrum of the doped $Ni_{0.4}M_{0.1}Zn_{0.5}Fe_2O_4$ samples (M represents Cu, Co, Ni, Mn, La respectively) obtained at 600 °C.

developed to synthesize nanoparticles of spinel ferrite. However, it is not easy to control the micro-morphology of the ferrite using the methods mentioned above. The preparation of one-dimensional (1D) nanostructured ferrites remains a challenge owing to the high symmetry of spinel structure which unfavorably induces 1D growth if there are no additional restrictions [17,18].

In this work, $FeCl_2$, $Ni(NO_3)_2$, $Zn(NO_3)_2$ and the precipitator (NaOH) were used for the preparation of the Zn- and Ni-doped spicular α-FeOOH precursor sample. $Ni_{0.5}Zn_{0.5}Fe_2O_4$ nanorods were obtained by the calcining of the precursor. Based on the $Ni_{0.5}Zn_{0.5}Fe_2O_4$ nanorods, $Ni_{0.4}M_{0.1}Zn_{0.5}Fe_2O_4$ (M represents Cu, Co, Mn, La) nanorods were prepared through the doping process. The effect of the dopant ions on the morphology, phase and the magnetic properties of the $Ni_{0.5}Zn_{0.5}Fe_2O_4$ nanorods was systemically studied.

2. Experimental

$FeCl_2$ (4 g) and polyglycol (0.5 g) were dissolved in deionized water and stirred continually in a magnetic blender at 50 °C. NaOH with the mass ratio of m(NaOH)/m($FeCl_2$) equal to 4 was dissolved in another deionized water. Subsequently, the NaOH solution was poured into the $FeCl_2$ solution to obtain intermixture A. According to the formula of $Ni_{0.4}M_{0.1}Zn_{0.5}Fe_2O_4$ (M represents Cu, Co, Mn, La), $Zn(NO_3)_2$, $Ni(NO_3)_2$ and $M(NO_3)_2$ were dissolved in appropriate quantities of deionized water to get intermixture B. The intermixture B was then dripped into the intermixture A using a perfusion tube. The dripping time was controlled at about 8 h. After the dripping process, the mixture was stirred continually for 5 h. Subsequently, the product was filtered and washed several times until the washing liquid was neutral. The precipitate was dried in the cabinet dryer at 80 °C to get the precursor samples. These precursor samples were calcined for 1 h at the temperature of 300 °C. Then, the products obtained were further calcined at 500, 600, and 700 °C respectively for 2 h. Finally, the $Ni_{0.4}M_{0.1}Zn_{0.5}Fe_2O_4$ samples were obtained.

The synthesized samples were subsequently characterized by X-ray diffraction (XRD, Rigaku D/max-gB X-ray diffractometer with Cu Kα radiation) and transmission electron microscope (TEM, H-800). The magnetic properties were measured using a vibrating sample magnetometer (VSM) at room temperature under a maximum field of 15 T.

3. Results and discussion

The phase identification of the precursor and the as-prepared $Ni_{0.4}M_{0.1}Zn_{0.5}Fe_2O_4$ samples was examined by XRD. Fig. 1 shows the XRD patterns of Cu-doped precursor and $Ni_{0.4}Cu_{0.1}Zn_{0.5}Fe_2O_4$ samples obtained at different calcination temperatures. These peaks are indexed to α-FeOOH phase according to the standard JCPDS, and no characteristic peaks of impurities (such as the peaks corresponding to $Ni(OH)_2$, $Cu(OH)_2$, $Zn(OH)_2$) are observed. A comparison of the $Ni_{0.4}Cu_{0.1}Zn_{0.5}Fe_2O_4$ samples obtained at different calcination temperatures shows that some α-Fe_2O_3 phase appeared in the samples calcined at the temperature lower than 600 °C. At 600 °C and above, all the observed peaks could be indexed as that of the spinel structure and no characteristic peaks of impurities were detected. The XRD patterns of the doped $Ni_{0.4}M_{0.1}Zn_{0.5}Fe_2O_4$ obtained at 600 °C are shown in Fig. 2. All the diffraction peaks in the XRD patterns could be perfectly indexed as spinel structure except that some characteristic peaks of La_2O_3 appeared in the XRD pattern of the La-doped samples. It is possibly due to the fact that the radius of La^{3+} is much higher than that of Ni^{2+}, so it is not easy for La^{3+} to enter into $Ni_{0.5}Zn_{0.5}Fe_2O_4$ and take up the position of Ni^{2+} to form spinel structure. Consequently, La^{3+} existed in the form of La_2O_3 in the samples.

The morphology and particle sizes of the precursor and the as-prepared $Ni_{0.4}M_{0.1}Zn_{0.5}Fe_2O_4$ samples were characterized by TEM. Fig. 3A and B shows respectively the TEM images of the precursor obtained without doping and $Ni_{0.5}Zn_{0.5}Fe_2O_4$ sample obtained at the calcination temperature of 600 °C. It can be seen from the TEM images that the morphology of the sample obtained without doping was rod-like. The average diameter of the precursor was 40 nm and the aspect ratio was 20. From the comparison of the precursor and the $Ni_{0.5}Zn_{0.5}Fe_2O_4$ sample, it can be found that though the length of the two samples may nearly be the same, the average diameter of the $Ni_{0.5}Zn_{0.5}Fe_2O_4$ was larger than that of the precursor, resulting in a decrease in the aspect ratio. The TEM images of the $Ni_{0.4}M_{0.1}Zn_{0.5}Fe_2O_4$ (M represents Cu, Co, Mn, La) obtained by the calcination of the Cu, Co, Mn, La doped precursor at 600 °C are shown in Fig. 3C–F, respectively. In contrast with the $Ni_{0.5}Zn_{0.5}Fe_2O_4$ sample, the $Ni_{0.4}Cu_{0.1}Zn_{0.5}Fe_2O_4$ and $Ni_{0.4}Co_{0.1}Zn_{0.5}Fe_2O_4$ samples were larger in length and their diameters decreased, resulting in an increase in the aspect ratio, which was higher than 25. However, the average diameter of the $Ni_{0.4}Mn_{0.1}Zn_{0.5}Fe_2O_4$ and $Ni_{0.4}La_{0.1}Zn_{0.5}Fe_2O_4$ was higher than that of the $Ni_{0.5}Zn_{0.5}Fe_2O_4$, which resulted in a decrease in the aspect ratio. The average diameter and length of $Ni_{0.4}La_{0.1}Zn_{0.5}Fe_2O_4$ were 60 and 500 nm, respectively. The aspect ratio of $Ni_{0.4}La_{0.1}Zn_{0.5}Fe_2O_4$ was 10. The TEM images of the $Ni_{0.4}Cu_{0.1}Zn_{0.5}Fe_2O_4$ obtained at the calcination temperatures of 500 and 700 °C are shown in Fig. 3G and H, respectively. As seen from the TEM images, the diameter of the $Ni_{0.4}Cu_{0.1}Zn_{0.5}Fe_2O_4$ samples increased with an increase in the temperature and the

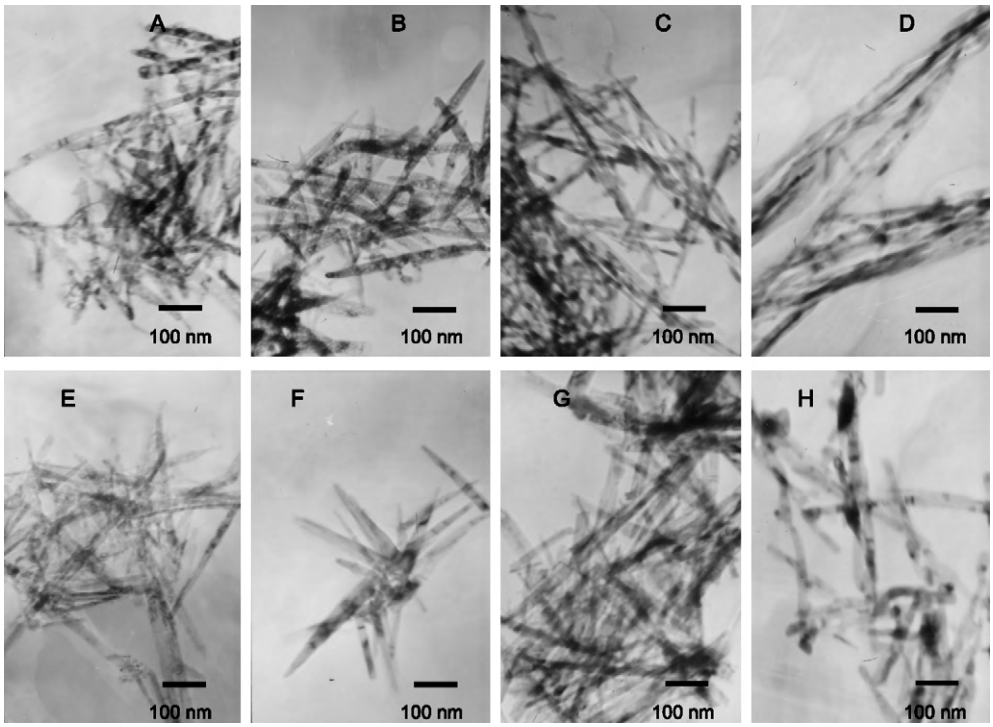

Fig. 3. The TEM images of the precursor and $Ni_{0.5}Zn_{0.5}Fe_2O_4$ samples.

crystal defect was found to appear in the rod-like samples obtained at the calcination temperature of 700 °C.

Goethite presented the orthorhombic *Pnma* space group and indicated that the unit cell contained four groups Me, O, OH [19]. The structure is based on an HCP packing of oxygen and hydroxide ions wherein half of the octahedral sites are filled with metal ions. The structure could be described as a series of double row octahedra that run parallel to (0 0 1); the double rows are separated by vacant double rows. Each octahedron in the double row shares two oxygen atoms from the same edge with two different octahedra from the same double row. Meanwhile, each octahedron shares two corners with two polyhedras from a neighboring double row. Such a structure indicates the presence of three different Me–Me distances. Thus, the external ion can enter the inside of α-FeOOH along three different directions to replace the position of Fe^{3+}. Moreover, the diameter and aspect ratio of α-FeOOH mainly depended on a preferential absorption of dopant ions on the surface of growing crystals at the plane perpendicular to the crystallographic different axis. If the dopant ion was preferentially absorbed in the *c*-axis direction, it would enter the inside of the crystal along the *c*-axis direction, and thereby the α-FeOOH particles would grow considerably in length (*c*-axis direction) with a suppressed growth in width and thickness (*a*- and *b*-axis directions, respectively). On the contrary, If the dopant ion was preferentially absorbed in the *a*- and *b*-axis directions, it would enter the inside of the crystal along the *a*- and *b*-axis directions to replace Fe^{3+}, which would decrease the step energy of growth and increase the crystal growth velocity of the *a*- and *b*-axis directions, resulting in an increase in the diameter of the α-FeOOH particles. It should be mentioned that the entry direction of the dopant ion depends mainly on the radius of the dopant ion [20]. Thus, the less the absolute difference of the radius of the dopant ion and Fe^{2+}, the more prone the dopant ion was to enter the α-FeOOH crystal lattice along the *c*-axis. As a result, the α-FeOOH samples with a smaller diameter and a higher aspect ratio were obtained. Betiana et al. [21] drew a similar conclusion in the preparation process of Co- or Mn-doped α-FeOOH sample. The corresponding ion radius of Fe^{2+}, Zn^{2+}, Cu^{2+}, Co^{2+}, Ni^{2+}, Mn^{2+} and La^{3+} irons were 0.74, 0.74, 0.72, 0.72, 0.69, 0.80 and 1.06, respectively [22]. The absolute difference order of the radius of the dopant ion and Fe^{2+} was as follows: $|r(La^{3+}) - r(Fe^{2+})| > |r(Mn^{2+}) - r(Fe^{2+})| > |r(Ni^{2+}) - r(Fe^{2+})| > |r(Co^{2+}) - rFe^{2+})| = |r(Cu^{2+}) - r(Fe^{2+})| > |r(Zn^{2+}) - r(Fe^{2+})|$ (*r* represents the radius of the ion). The particle size and aspect ratio of the $Ni_{0.4}M_{0.1}Zn_{0.5}Fe_2O_4$ (M represents Cu, Co, Mn, La) obtained via the coprecipitation method depended on the particle size and aspect ratio of M-doped α-FeOOH. Thus, it can be concluded that the aspect ratio of the $Ni_{0.4}M_{0.1}Zn_{0.5}Fe_2O_4$ decreased with an increase in the absolute difference of the radius of the dopant ion and Fe^{2+}.

Table 1 shows the magnetic properties of $Ni_{0.5}Zn_{0.5}Fe_2O_4$ and $Ni_{0.4}M_{0.1}Zn_{0.5}Fe_2O_4$. As seen in Table 1, there is a reduction in coercivity with an increase in calcination temperature of the ferrites. The $Ni_{0.5}Zn_{0.5}Fe_2O_4$ sample obtained at the calcination temperature of 500 °C, whose coercivity, saturation magnetization and

Table 1
Magnetization measurement of the as-prepared $Ni_{0.4}M_{0.1}Zn_{0.5}Fe_2O_4$ samples.

X	*T* (°C)	Hc (Oe)	Ms (emu/g)	Mr (emu/g)
$Ni_{0.5}Zn_{0.5}Fe_2O_4$	500	132.3	8.6	2.1
	600	90.5	39.7	8.1
	700	70.2	45.3	8.0
$Ni_{0.4}Cu_{0.1}Zn_{0.5}Fe_2O_4$	500	179.4	25.3	8.2
	600	91.2	41.5	9.5
	700	87.4	64.3	12.9
$Ni_{0.4}Co_{0.1}Zn_{0.5}Fe_2O_4$	500	185.3	22.7	6.9
	600	94.2	46.4	6.4
	700	85.6	62.2	14.0
$Ni_{0.4}Mn_{0.1}Zn_{0.5}Fe_2O_4$	500	169.4	18.3	7.2
	600	90.3	52.6	7.4
	700	68.7	57.7	7.7
$Ni_{0.4}La_{0.1}Zn_{0.5}Fe_2O_4$	500	220.6	10.7	5.3
	600	71.2	28.9	5.6
	700	50.5	32.8	7.0

remanent magnetization are 132.3 Oe, 8.6 and 2.1 emu/g respectively, exhibited the properties of hard magnetism due to the presence of the rod-like α-Fe_2O_3 phase. The coercivity is found to be close to that of rod-like α-Fe_2O_3 reported in Ref. [23]. However, the magnetization improved on account of the existence of the $Ni_{0.5}Zn_{0.5}Fe_2O_4$ phase in the sample. With the increase in calcination temperature, the coercivity of the samples decreased while the magnetization further improved. The variation in magnetization with an increase in calcination temperature could be attributed to the following factors: better crystal structure perfection, increase in sample density, reduction in the shift resistance of the magnetic domain, the strength of the magnetism transfer effect and so on. The doped samples showed similar trend in coercivity and magnetization with an increase in calcination temperature. In general, the coercivity of the $Ni_{0.4}M_{0.1}Zn_{0.5}Fe_2O_4$ samples calcined at 500 °C is higher than that of the undoped ferrite. This is possibly due to the presence of the α-Fe_2O_3 phase in the doped samples obtained at 500 °C. The $Ni_{0.4}M_{0.1}Zn_{0.5}Fe_2O_4$ samples calcined at 600 °C did not show a significant variation in coercivity with change in radius of the dopant ion except for the La-doped sample. The lower coercivity in the La-doped sample could be attributed to the existence of the La_2O_3 phase. In case of the doped samples calcined at 700 °C, a decreasing trend in the coercivity with the increase in the absolute difference of radius of dopant ion and Fe^{2+} is observed. This shows a decrease in anisotropy in the $Ni_{0.4}M_{0.1}Zn_{0.5}Fe_2O_4$ samples with increasing radius of the dopant ion. The $Ni_{0.5}Zn_{0.5}Fe_2O_4$ with irregular shapes and sizes ranging from 10 to 30 nm obtained by the coprecipitation method in Ref. [24] exhibited lower coercivity (10–20 Oe) compared to the values of our samples annealed at 600 °C. This is indicative of the higher magnetocrystalline anisotropy possessed by the present samples. The differences in magnetocrystalline anisotropy should be mainly attributed to the differences in particle morphology [25]. As the presence of shape anisotropy can significantly enhance the magnetic properties [26], a higher aspect ratio, resulting in a higher shape anisotropy, can favor the increase of the coercivity.

4. Conclusions

The rod-like nano-$Ni_{0.5}Zn_{0.5}Fe_2O_4$ with a grain size of 40 nm and an aspect ratio of 20 was prepared after the calcination of the rod-like precursor. $Ni_{0.5}Zn_{0.5}Fe_2O_4$ was doped with Cu, Co, Mn and La to prepare rod-like nano-$Ni_{0.4}M_{0.1}Zn_{0.5}Fe_2O_4$ (M represents Cu, Co, Mn, La). The results from TEM and VSM indicated that the effect of the dopant ion on the morphology of $Ni_{0.4}M_{0.1}Zn_{0.5}Fe_2O_4$ depended on the absolute difference of the radius of the dopant ion and Fe^{2+}. The aspect ratio of the $Ni_{0.4}M_{0.1}Zn_{0.5}Fe_2O_4$ was found to decrease with the increase in the absolute difference of the radius of the dopant ion and Fe^{2+}. For the sample obtained with the same dopant iron, the diameter of the $Ni_{0.4}M_{0.1}Zn_{0.5}Fe_2O_4$ nanorods increased, the length of sample reduced, the coercivity decreased and the magnetization increased with an increase in calcination temperature. The magnetic properties of the present samples are superior to those reported for ferrites with irregular grain shapes and can be attributed to the higher anisotropy of the nanorods.

Acknowledgments

The authors acknowledge the North University of China for the support given for carrying out this work under projects from the National Natural Science Fund (20871108) and the returned overseas student fund projects of Shanxi province (200712011).

References

[1] M.M. Rashad, E.M. Elsayed, M.M. Moharam, et al., J. Alloys Compd. 486 (2009) 759–767.
[2] D.L. Zhao, Q. Lv, Z.M. Shen, J. Alloys Compd. 480 (2009) 634–639.
[3] Q. Song, Z.J. Zhang, J. Am. Chem. Soc. 126 (2004) 6164–6168.
[4] X. Li, G. Wang, J. Magn. Magn. Mater. 321 (2009) 1276–1279.
[5] C.R. Vestal, Q. Song, Z.J. Zhang, J. Phys. Chem. B 108 (2004) 18222–18227.
[6] J. Shi, S. Gider, K. Babcock, D.D. Awschalom, Science 271 (1996) 937–941.
[7] A.M.M. Farea, S. Kumar, K.M. Batoo, J. Alloys Compd. 469 (2009) 451–457.
[8] M.N. Ashiq, N. Bibi, M.A. Malana, J. Alloys Compd. 490 (2010) 594–597.
[9] M.K. Shobanaa, S. Sankara, V. Rajendranb, Mater. Chem. Phys. 113 (2009) 10–13.
[10] L.M. Dong, Z.D. Han, Y.M. Zhang, J. Rare Earth S1 (2006) 54–56.
[11] C. Venkataraju, G. Sathishkumar, K. Sivakumar, J. Magn. Magn. Mater. 322 (2004) 230–233.
[12] S.M. Li, Q. Wang, A.B. Wu, Curr. Appl. Phys. 9 (2009) 1386–1392.
[13] A.C.F.M. Costa, A.M.D. Leite, H.S. Ferreira, J. Eur. Ceram. Soc. 28 (2008) 2033–2037.
[14] S. Dasgupta, K.B. Kim, J. Ellrichc, et al., J. Alloys Compd. 424 (2006) 13–20.
[15] M. Gharagozlou, J. Alloys Compd. 486 (2009) 660–665.
[16] J.L. Zhang, J.X. Shi, M.L. Gong, J. Solid State Chem. 182 (2009) 2135–2140.
[17] Z.Y. Lai, Y.L. Zheng, J. Funct. Mater. 5 (2007) 833–835.
[18] F.F. Liu, X.Y. Li, Q.D. Zhao, H. Yang, Q. Xie, Acta Mater. 57 (2009) 2684–2690.
[19] S.K. Kwon, S. Suzuki, M. Saito, Corros. Sci. 47 (2005) 2543–2549.
[20] M. Alvarez, E.E. Sileo, E.H. Rueda, Am. Miner. 93 (2008) 584–590.
[21] B.C. Campo, O. Rosseler, M. Alvarez, Mater. Chem. Phys. 109 (2008) 448–454.
[22] Y.L. Chi, Inorganic Chemistry, Higher Education Press, Beijing, 2001.
[23] X.J. Zhang, Q.L. Li, Mater. Lett. 62 (2008) 988–990.
[24] M. Jalaly, M.H. Enayati, F. Karimzadeh, J. Alloys Compd. 480 (2009) 737–740.
[25] D. Li, T. Herricks, Y. Xia, Appl. Phys. Lett. 83 (2003) 4586–4588.
[26] E.E. Carpenter, C.J. O'Connor, V.J. Harris, J. Appl. Phys. 85 (1999) 5175–5179.